

NMRlipids IV: Headgroup & glycerol backbone structures, and cation binding in bilayers with PE and PG lipids

Amélie Bacle,¹ Pavel Buslaev,² Rebeca García Fandiño,^{3,4} Fernando Favela-Rosales,⁵ Tiago Ferreira,⁶ Patrick Fuchs,¹ Matti Javanainen,⁷ Anne M. Kiirikki,⁸ Jesper J. Madsen,^{9,10} Josef Melcr,^{7,11} Paula Milan Rodriguez,¹ Markus S. Miettinen,¹² O. H. Samuli Ollila,^{8,*} Chris G. Papadopoulos,¹³ Antonio Peón,¹⁴ Thomas J. Piggot,¹⁵ and Ángel Piñeiro¹⁶

¹Paris, France

²University of Jyväskylä

³Center for Research in Biological Chemistry and Molecular Materials (CiQUS),
Universidade de Santiago de Compostela, E-15782 Santiago de Compostela, Spain

⁴CIQUP, Centro de Investigação em Química, Departamento de Química e Bioquímica,
Faculdade de Ciências, Universidade do Porto, Porto, Portugal

⁵Departamento de Ciencias Básicas, Tecnológico Nacional de México, Campus Zacatecas Occidente, México

⁶Halle, Germany

⁷Institute of Organic Chemistry and Biochemistry of the Czech Academy of Sciences,
Flemingovo nám. 542/2, CZ-16610 Prague 6, Czech Republic

⁸Institute of Biotechnology, University of Helsinki

⁹Department of Chemistry, The University of Chicago, Chicago, Illinois, United States of America

¹⁰Department of Global Health, College of Public Health,

University of South Florida, Tampa, Florida, United States of America

¹¹Groningen Biomolecular Sciences and Biotechnology Institute and The Zernike Institute for Advanced Materials,
University of Groningen, 9747 AG Groningen, The Netherlands

¹²Department of Theory and Bio-Systems, Max Planck Institute of Colloids and Interfaces, 14424 Potsdam, Germany

¹³I2BC - University Paris Sud

¹⁴Spain

¹⁵Chemistry, University of Southampton, Highfield, Southampton SO17 1BJ, United Kingdom

¹⁶Departamento de Física Aplicada, Faculdade de Física,
Universidade de Santiago de Compostela, E-15782 Santiago de Compostela, Spain

(Dated: March 3, 2021)

Chemistry of lipid headgroups, the water facing components of cell membranes that regulate cell functions via lipid–protein interactions, varies between organisms and organelles. Because lipid membranes are in liquid state under physiological conditions, the conformational ensembles of different lipid headgroups are difficult to resolve experimentally. Here, we combine solid state NMR experiments and molecular dynamics simulations from NMRlipids open collaboration to resolve the conformational ensembles of the headgroups of key lipid types in liquid lamellar phase under various biologically relevant conditions. Interpretation of NMR experiments using the plethora of simulation data collected in the NMRlipids project suggests that all lipid headgroups sample a wide range of conformations in neutral and charged cellular membranes. However, the populations of different conformations are dictated by the headgroup chemistry. Together with the analysis of protein-bound lipids from the protein data bank (PDB), this suggests that lipids can bind to proteins in wide range of conformations independently on the headgroup chemistry. Therefore, the selective adsorption of proteins to membranes is likely regulated by specific protein–lipid interactions, rather than conformational restrictions of lipids. Our results pave the way to comprehensive understanding of lipid–protein interaction energetics, and the understanding of complex biomolecular assemblies such as membrane proteins.

INTRODUCTION

Chemical compositions of hydrophilic lipid headgroups vary between different organelles and organisms, and different lipid types regulate protein functions in many different ways [1, 2]. Lipids can directly bind to proteins or indirectly affect protein functions by altering membrane properties such as charge or elasticity [1, 3]. While the specific interactions with certain lipid headgroups are known to be essential for the function of several proteins [3, 4], it is not clear if the specificity is driven by the differences in accessible conformational states between lipid types or by specific intermolecular lipid–protein interactions.

The conformational ensembles of lipids in the physiologi-

cally relevant lamellar liquid phase are typically derived from NMR experiments, particularly from C–H bond order parameters measured using ²H NMR [5–7]. Notably, such measurements can be performed also on living cells [8–10]. These studies suggest that the glycerol backbone conformations are largely similar irrespectively of the headgroup [8], and the headgroup conformations are similar in phosphatidylcholine (PC), phosphatidylethanolamine (PE) and phosphatidylglycerol (PG) lipids, while the headgroup is more rigid in phosphatidylserine (PS) lipids [11, 12]. However, these tendencies are based only on the absolute values, whereas the necessity of order parameter signs in capturing the conformational ensembles of lipids has been recently demonstrated [13–15]. Furthermore, the detailed understanding of lipid conformational ensembles is limited by the lack of universal models that

would map order parameters to structural ensembles [16, 17].

Structures of different lipid types in protein bound states can be extracted from the protein data bank (PDB) [18], but their relation to the conformational ensembles in liquid lamellar state remains unclear [19]. In addition to the changes in lipid conformational ensembles upon binding to proteins, also the experimentally measured response of lipid headgroup to membrane bound charges remains poorly understood due to the lack of suitable models to interpret the lipid conformational ensembles in liquid lamellar state [7].

Here, we use natural abundance ^{13}C NMR experiments and MD simulations from the NMRlipids open collaboration to resolve the differences in conformational ensembles between PC, PE, PG and PS lipid headgroups. Zwitterionic PC and PE are the most common lipids in eukaryotes and bacteria, respectively [2, 20]. PE is also the second most abundant glycerophospholipid in eukaryotic cells and has been related to various diseases [21–23]. PS and PG are the most common negatively charged lipids in eukaryotes and bacteria, respectively, and affect membrane protein functionality and signaling [3, 20, 24, 25]. All the studied lipids specifically bind to various proteins [26]. We use our results to elucidate also lipid–protein interactions and the effect of charges on lipid conformations.

The lipid conformational ensembles in liquid lamellar state paves the way toward understanding the specific binding of different lipid types to membrane proteins and how they regulate the protein function. Because glycerol backbone and headgroup structures of PC lipids are similar in model membranes and in bacteria [8–10], the results from model systems could be used to understand the biological role of lipid headgroup conformational ensembles in different lipid types.

METHODS

Experimental C–H bond order parameters

The headgroup and glycerol backbone C–H bond order parameters of 1-palmitoyl-2-oleoyl-sn-glycero-3-phosphoethanolamine (POPE) and 1-palmitoyl-2-oleoyl-sn-glycero-3-phospho-(1'-rac-glycerol) (POPG), purchased from Avanti polar lipids, were measured using natural abundance ^{13}C solid state NMR spectroscopy as described previously [15, 27]. The magnitudes of order parameters were determined from the chemical-shift resolved dipolar splittings using a R-type Proton Detected Local Field (R-PDLF) experiment [28] and the signs from S-DROSS experiments [29] combined with SIMPSON simulations [30]. The NMR experiments were identical as in our previous work [31]. The POPE experiments were recorded at 310 K and POPG experiments at 298 K, where the bilayers are in the liquid disordered phase [32].

Glycerol backbone peaks from both lipids, and α -carbon peak from POPE in the INEPT spectra were assigned based on previously measured POPC spectra [27]. The β -carbon peak

from POPE was assigned based on ^{13}C chemical shift table for amines available at <https://www.chem.wisc.edu/areas/reich/nmr/c13-data/cdata.htm>. **1.How were α and γ -carbon peaks assigned in POPG?** The β -carbon peak from POPG overlapped with the g_2 peak from glycerol backbone because their chemical environments are similar. **2.Details to be checked by Tiago.**

Molecular dynamics simulations

Molecular dynamics simulation data were collected and analyzed using the methods from the NMRlipids Open Collaboration project (nmrlipids.blogspot.fi) [13, 14, 31, 33]. Simulation and accessibility details of more than 70 systems simulated for this work are given in the supplementary information. Quality evaluation of these simulations enables us to select the best models for the interpretation of lipid conformational ensembles from the experimental data.

The quality of lipid headgroup and glycerol backbone conformational ensembles in PE and PG simulations were evaluated using the C–H bond order parameters [13]. Interactions between different headgroups in simulations of mixed bilayers were evaluated monitoring the changes in headgroup order parameters upon mixing the lipids [31]. The ion binding affinities and response of lipids to bound charge were evaluated monitoring the changes of lipid headgroup order parameters [31, 33].

Analysis of conformations of protein-bound lipids

4.This is to be finished once the final analysis is done as discussed in this issue:
<https://github.com/NMRlipids/NMRlipidsIVPEandPG/issues/40>

Lipid structures from Protein Data Bank (PDB, <http://www.rcsb.org/>) were searched using PDB REST API (www.ebi.ac.uk/pdbe/pdbe-rest-api). First, all PDB entries containing PC, PE, PG, or PS lipid headgroups were collected. The ligand names to identify the lipids were: PLC, PX4, 6PL, LIO, HGX, PC7, PC8, P1O, 6O8, XP5, EGY, PLD, SBM, HXG, and PCW for PC; 8PE, PTY, 3PE, PEH, PEF, 6OE, 6O9, 9PE, PEV, 46E, SBJ, L9Q, PEK, EPH, ZPE, 9TL, 9Y0, 6OU, LOP, and PEE for PE; PGT, PGK, LHG, 44G, PGV, OZ2, D3D, PGW, DR9, P6L, PG8, H3T, and GOT for PG; and PSF, PS6, Q3G, P5S, D39, PS2, 17F, and 8SP for PS. Secondly, all PDB structures containing these ligands were downloaded and the dihedral angles of the first lipid in the latest version of the structures within each PDB code were calculated using the MDTraj python library [37]. The used Jupyter notebook is available from the project's GitHub repository ([scripts/pdbSEARCH.ipynb](https://github.com/NMRlipids/NMRlipidsIVPEandPG/blob/master/scripts/pdbSEARCH.ipynb)).

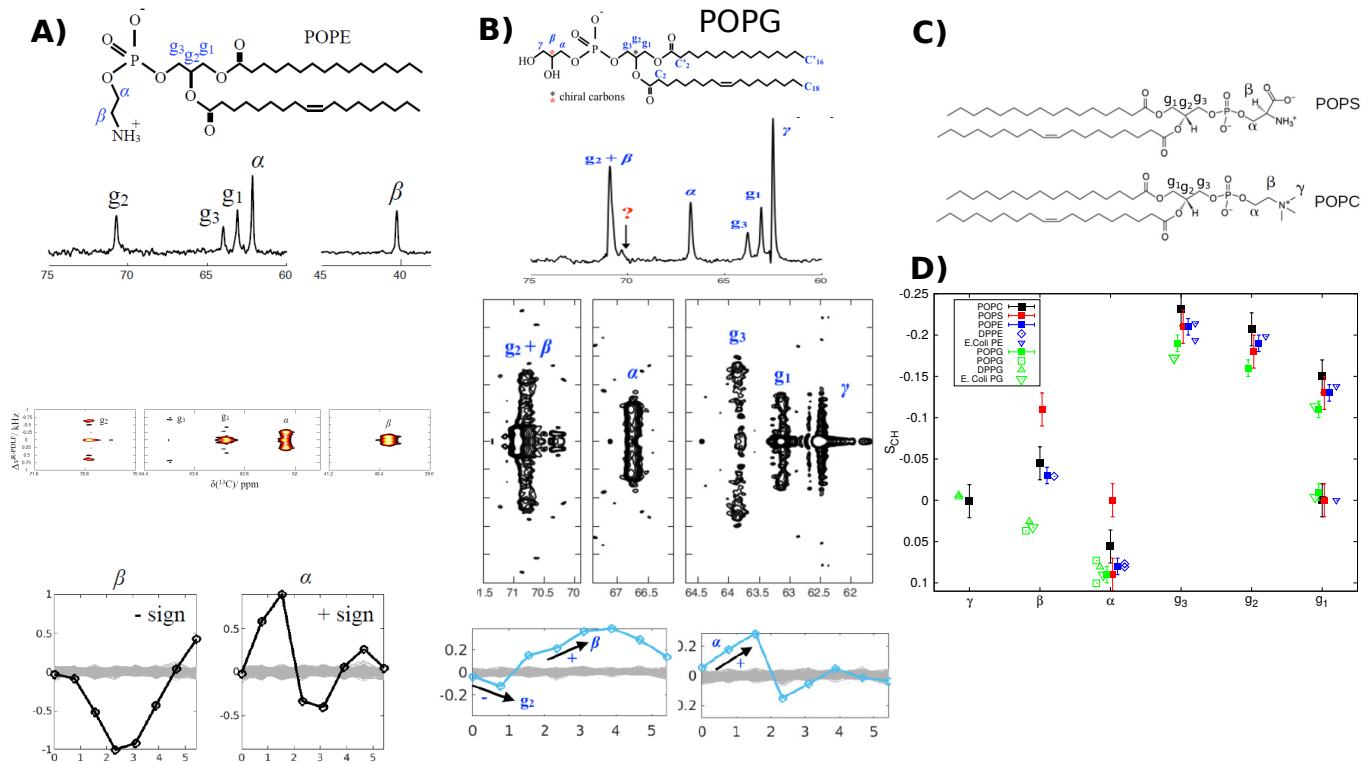


FIG. 1: Chemical structure, refocused-INEPT spectrum, 2D R-PDLF spectra, and S-DROSS data (from top to bottom) of **A)** POPE and **B)** POPG. Full NMR spectra are shown Figs. S1 and S2. **C)** Chemical structure of POPC and POPS. **D)** Headgroup and glycerol backbone order parameters from different experiments in lamellar liquid disordered phase. The values and signs for POPE (310 K) and POPG (298 K) measured in this work, and for POPS (298 K) [31] and POPC (300 K) [15, 27] previously using ^{13}C NMR. The literature values for DOPS with 0.1M of NaCl (303 K) [34], POPG with 10mM PIPES (298 K) [35], DPPG with 10mM PIPES and 100mM NaCl (314 K) [11], DPPE (341 K) [36], E.coliPE and E.coliPG (310 K) [8] are measured using ^2H NMR. The signs from ^{13}C NMR are used also for the literature values.

3.This is a sketch, Tiago Ferreira will make a new figure.

RESULTS AND DISCUSSION

Differences between lipid headgroups in bulk bilayer from ^{13}C NMR experiments

To experimentally characterize the headgroup conformational ensembles of lipids that are not bound to proteins in an electrostatically neutral cell membrane, we measured the C–H bond order parameters and their signs of POPG and POPE in the liquid lamellar phase, as we did previously for POPC and POPS [15, 27, 31]. Determination of headgroup and glycerol backbone order parameters and their signs was straightforward from the data in Figs. 1, S1 and S2 for all the C–H bonds, except for the β and g_2 carbons in POPG. These carbons have overlapping peaks in the INEPT spectra due to their similar chemical environments, and only the magnitude of the larger order parameter could be determined from the R-PDLF spectra (Fig. 1B)). Nevertheless, based on previous ^2H NMR measurements [8, 11, 35], we assigned the larger order parameter to the g_2 carbon and used the literature value for the β -carbon in SIMPSON simulations to determine the signs. The decrease in the beginning of the S-DROSS curve suggests that the sign of larger g_2 order parameter is negative

and later increase suggests that sign of smaller β order parameter is positive (Fig. 1B)). This interpretation is confirmed by SIMPSON calculations in Fig. S3.

Experimental order parameters of POPC, POPE, POPG and POPS glycerol backbones and headgroups from this and previous studies are collected in Fig. 1D), where signs determined from ^{13}C NMR experiments are used also for the ^2H NMR data from the literature. The overall agreement of order parameters determined by different research teams and different techniques for the same lipid headgroup is very good here and in previous studies [13, 14, 31]. This suggests that the observed differences between lipid types arise from differences in headgroup chemistry rather than inaccuracies in experiments, or differences in the acyl chains or in experimental conditions. The most distinct order parameters are observed for PS headgroups, for which the α -carbon order parameter exhibits significant forking and the β -carbon has more negative value than other studied lipid types. On the other hand, the β -carbon order parameter of PG headgroup has a positive sign, in contrast to all the other lipid types. Notably, this has not been observed in traditional ^2H NMR experiments, where only the absolute value of the order parameters are measured [8, 11, 35]. The glycerol backbone order parameters are

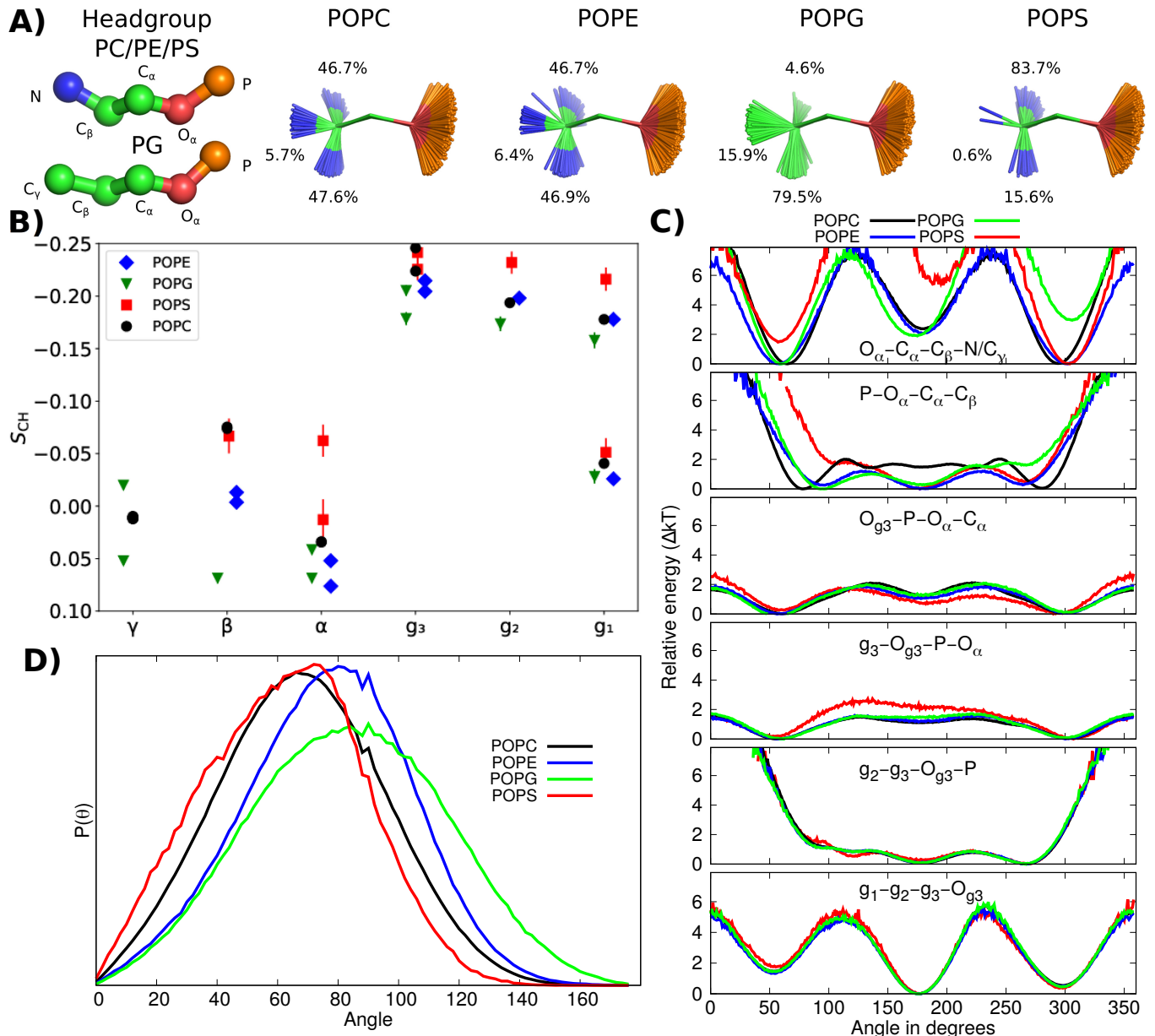


FIG. 2: Results from the best simulation model (CHARMM36) simulations demonstrating the differences in conformational ensembles between different lipids. **A)** Snapshots with overlaid C_{β} , C_{α} and O_{α} atoms and occurrence of different conformations. **B)** Headgroup and glycerol backbone region order parameters of different different lipids. **C)** Relative energies for individual dihedral angles estimated from inverse Boltzmann distributions of heavy atom dihedral angles. The states corresponding energies higher than 7 kT are not shown because they are not observed in simulations. **D)** Distributions of P-N vector angle with respect to membrane normal.

similar for all the lipid types, although they move slightly toward positive values (closer to zero) in the order $PC < PE < PS < PG$. Essential differences between PC and PE headgroups are not observed.

Conformational ensembles of different lipid headgroups in bulk bilayer from MD simulations

To understand the structural origin of distinct order parameters for PG and PS lipids, we first calculated the heavy atom dihedral angle distributions from simulations that best reproduce the differences between headgroups according to the quality evaluation in the SI and Refs. [13, 31] (Fig. S12). Then, we used the inverse Boltzmann distributions to estimate the energy costs for different dihedral angle orientations. The

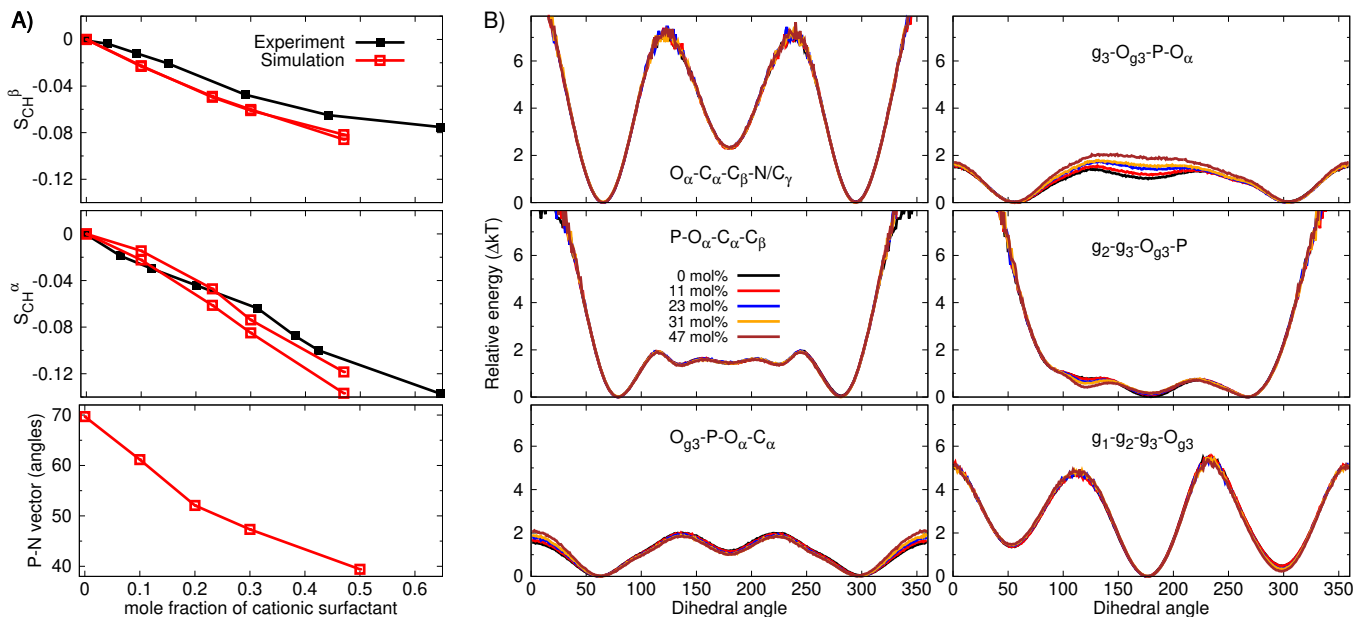


FIG. 3: **A)** Modulation of PC headgroup order parameters and P-N vector angle upon addition of cationic surfactant from CHARMM36 simulations compared with the experimental data [38]. **B)** Relative energies for individual dihedral angles estimated from inverse Boltzmann distributions of heavy atom dihedral angles with different amounts of cationic surfactant from CHARMM36 simulations.

results in Fig. 2C) suggest that all lipid headgroups are very flexible and energy costs for rotating individual dihedrals to almost any angle is low (below 7 kT). Only trans states of $P-O_{\alpha}-C_{\alpha}-C_{\beta}$ and $g_2-g_3-O_{g3}-P$ have larger relative energies and are not observed for any lipids during the simulations.

Major differences between headgroups are observed for the last two dihedrals in the headgroup end, $O_{\alpha}-C_{\alpha}-C_{\beta}-N/C_{\gamma}$ and $P-O_{\alpha}-C_{\alpha}-C_{\beta}$, which prefer *gauche*⁻ conformations for PG and *gauche*⁺ for PS, while PC and PE exhibit symmetric distributions. Also, the energy barriers for $O_{\alpha}-C_{\alpha}-C_{\beta}-N/C_{\gamma}$ dihedral rotations between *gauche* and *trans* states are larger for PS and PG lipids than for PC and PE lipids. Rest of the dihedrals are similar between different lipids, with the exception of PS lipids for which slightly larger energy for eclipsed anti conformation in $g_3-O_{g3}-P-O_{\alpha}$ dihedral was observed. Therefore we suggest that the main differences between lipid headgroups leading to distinct order parameter occur in the choline part, while also changes in phosphate region may contribute in PS lipids. The increased barriers for dihedral rotations may explain the more rigid headgroup structures in PS [12, 34]. Furthermore, the angle between headgroup dipole and membrane normal decreases in the order of PG > PE > PC > PS (Fig. 2D)). However, the differences between PC and PE in $P-O_{\alpha}-C_{\alpha}-C_{\beta}$ dihedral and P-N vector dipole may be artificial as the β -carbon order parameter in PC is too negative in the CHARMM36 force field, thereby not being equal to the order parameter in PE as observed in experiments [13].

In conclusion, all lipid headgroups sample very broad conformational ensembles in liquid lamellar phase and sampled dihedral angles are within approximately same ranges for all headgroup types. Because the rotation of dihedral angles

to almost any position bears relatively low energy cost, the lipid headgroups are able to adopt wide range of multiple conformations when interacting with proteins, ions or other biomolecules. The wide range of observed conformations suggest that the structures in lipid crystals [12, 39] play only a minor role, and that the models aiming to explain NMR data using only few conformations [5–7, 17] are not sufficient to capture the large conformational space of lipids in liquid lamellar state.

Lipid conformational ensembles in lipid bilayers with bound ions

Charged entities, such as lipids, proteins, surfactants, drugs, and ions incorporated in membranes reorient the headgroup dipole in PC lipids, thereby affecting the order parameters of lipid headgroups [40]. However, the detailed understanding on structural and energetic response of lipids to membrane bound electric charge is still lacking [7].

To resolve lipid headgroup conformational ensembles in cell membrane bearing positive charge, we calculated the heavy atom dihedral angle distributions from simulations that correctly captured the experimentally measured decrease in PC headgroup order parameters upon addition of cationic surfactants into a bilayer in figure 3 A). The dihedral angle distributions and relative energies in figures S13 and 3 B reveal that the addition positive charge into a membrane decrease the abundance of trans states in $g_2-g_3-O_{g3}-P$ and $g_3-O_{g3}-P-O_{\alpha}$ dihedrals. Choline region remains essentially unchanged and only minor changes are observed in other dihedrals even

though almost half of the molecules in membranes are cationic surfactants.

Also binding of ions to membranes may affect the lipid headgroup conformational ensembles in physiological conditions. The bound Ca^{2+} ion to PC headgroup leads to similar decrease in trans state probability for $\text{g}_3\text{-O}_{\text{g}_3}\text{-P-O}_{\alpha}$ dihedral as observed for cationic surfactants in the most realistic MD simulations models (lipid17ecc and CHARMM36 in Figs. S14, S15 and Fig. S8). The dihedral distributions of PG headgroup are more sensitive to the bound ions in the most realistic simulations, but upward tilting of the headgroup dipole upon addition of CaCl_2 is weaker than in PC (Lipid17 and Slipids in Figs. S8, S16 and S17). However, the changes in PG lipid dihedrals upon addition of CaCl_2 differ between the best models (Figs. S16 and S17), none of the simulations captures the Ca^{2+} ion binding affinity and conformational ensemble of PG lipids simultaneously, and experimental data to evaluate the response of α -carbon order parameters to the added CaCl_2 in PG is not available. Also the headgroup conformational ensembles in mixtures of PC and charged (PG or PS) or zwitterionic (PE) lipids could not be resolved with the currently available force fields and experimental data (Figs. S6 and S7, and Ref. [31, 41]).

Despite the difficulties in simulations to capture the headgroup conformations in mixtures involving charged lipids, we can conclude that the structural response of lipid headgroups to membrane bound charges arise from relatively small changes in conformational ensembles. These changes eventuate from mild changes in dihedral angle distributions, rather than from restriction of lipids into fixed conformations. Therefore, lipid headgroups remain in disordered state sampling large space of different conformations also in charged membranes, thereby being able to interact with different molecules in multiple ways.

Protein-bound lipid conformations

To analyze the alterations in lipid conformations when bound to proteins, we calculated the heavy atom dihedral distributions from lipid conformations within protein structures deposited in the PDB [18] in Fig. 4. **5.This part is to be finished once the analysis is finalized** We found 176 PC, 198 PE, 70 PG, and 41 PS conformations, which present lipids that are tightly bound to proteins in fixed conformations that can be determined as a part of protein structure using crystallography or cryo-EM.

Similarly to the liquid lamellar state, lipid dihedrals have very wide range of angles when bound to proteins. Only $\text{P-O}_{\alpha}\text{-C}_{\alpha}\text{-C}_{\beta}$ and $\text{g}_2\text{-g}_3\text{-O}_{\text{g}_3}\text{-P}$ dihedrals seem to avoid *cis* conformations as observed also in liquid lamellar state. The $\text{O}_{\alpha}\text{-C}_{\alpha}\text{-C}_{\beta}\text{-N/C}_{\gamma}$ and $\text{g}_1\text{-g}_2\text{-g}_3\text{-O}_{\text{g}_3}$ dihedrals are even less restricted in protein bound state than in liquid lamellar phase where *cis* and *anti* eclipsed state were not present (Fig. 2). Major differences between different lipid headgroups are not observed when bound to proteins. Slight preference for the trans state in $\text{O}_{\alpha}\text{-C}_{\alpha}\text{-C}_{\beta}\text{-C}_{\gamma}$ dihedral of PC, and for positive

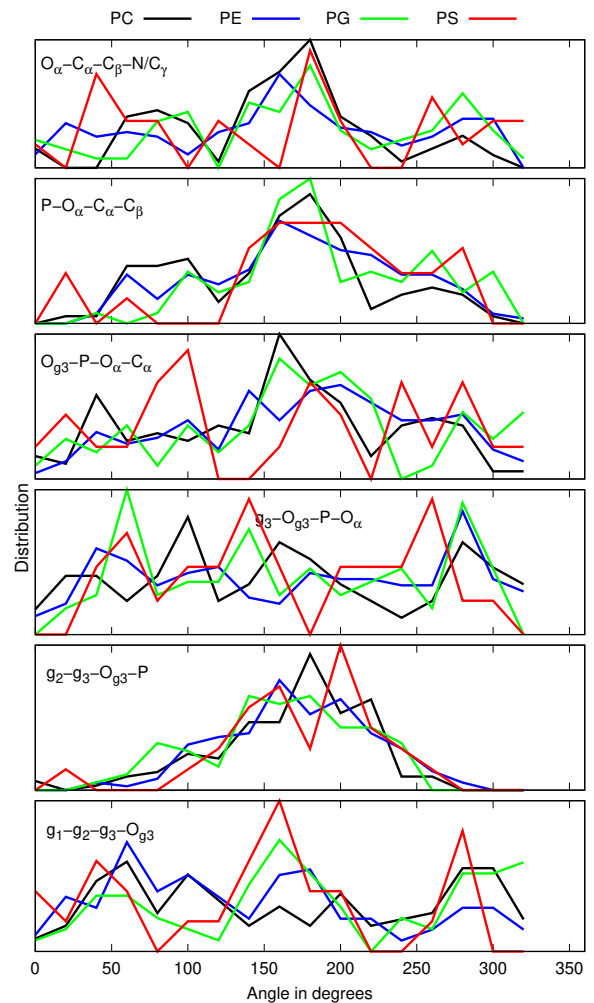


FIG. 4: Dihedral distributions from simulations and lipid structures in PDB.

angles in $\text{P-O}_{\alpha}\text{-C}_{\alpha}\text{-C}_{\gamma}$ dihedral of PS lipids with respect to other lipids could be present in the data, but the statistics is not sufficient for conclusions. Therefore, the differences in conformational ensembles between different lipids in liquid lamellar state in Fig. 2 are not seen in the protein bound states.

This suggests that lipids can bind to proteins in wide range of conformations independently of headgroup chemistry. Thereby, lipids compromise their preferred conformations when binding to proteins and the binding of lipids to specific locations would be driven by the intermolecular interactions between proteins and lipids. However, it is important to note that lipids are often not the main target in structures deposited in PDB and therefore their conformations may be less reliable than those of proteins. Stereochemical violations and structures deviating from lipid crystals have been previously proposed to indicate inaccuracies in lipid structures in PDB [16, 19]. However, we see large deviations from lipid crystals structures also in conformational ensembles that reproduce the NMR data in liquid lamellar phase, thereby proposing that such deviations are realistic also in protein-bound states.

CONCLUSIONS

Conformational ensembles resolved using solid state NMR experiments and MD simulations from NMRlipids open collaboration revealed that headgroups of the most abundant biological phospholipids, PC, PE, PG and PS, sample a wide range of different conformations in the lamellar liquid state. Differences in NMR order parameters between different headgroups can be explained by the changes in dihedral angle distributions, suggesting that similar conformations are accessed by all headgroups, but with different probabilities. Also the changes in order parameters upon the addition of charged molecules—such as cationic lipids, surfactants, or drugs—in membranes can be explained by the changes in dihedral angle probabilities, particularly close to the phosphate region.

Wide range of conformations are observed also in lipids that are tightly bound to proteins in PDB, suggesting that the specific binding of lipids to proteins is dominated by the intermolecular lipid–protein interactions, while the differences in conformational ensembles between different lipid types play a minor role. Therefore, lipids can conform themselves to multiple binding positions located in various proteins.

Our results pave the way to understanding how lipids regulate membrane protein function. Lipid conformational ensembles in liquid lamellar phase are necessary for the detailed analysis of lipid–protein interaction energetics, particularly for its entropic component. Furthermore, our results demonstrate how the NMRlipids databank, containing MD simulations and NMR data, can be used to resolve conformational ensembles of disordered biomolecules in a membrane environment, and how this information can be coupled with structural data in the PDB. We believe that this combination brings us closer to the comprehensive understanding of complex biomolecular assemblies containing both disordered and structural regions, such as membrane protein complexes.

AP is grateful to the Centro de Supercomputacin de Galicia (CESGA) for use of the Finis Terrae computer

* samuli.ollila@helsinki.fi

- [1] A. Lee, *Biochimica et Biophysica Acta (BBA) - Biomembranes* **1612**, 1 (2003), ISSN 0005-2736, URL <http://www.sciencedirect.com/science/article/pii/S0005273603000567>.
- [2] G. van Meer, D. R. Voelker, and G. W. Feigenson, *Nature Reviews Molecular Cell Biology* **9**, 112 (2008), URL <https://doi.org/10.1038/nrm2330>.
- [3] M. A. Lemmon, *Nat. Rev. Mol. Cell Biol.* **9**, 99 (2008).
- [4] A. G. Lee, *Trends in Biochemical Sciences* **36**, 493 (2011), URL <https://doi.org/10.1016/j.tibs.2011.06.007>.
- [5] J. Seelig, *Q. Rev. Biophys.* **10**, 353 (1977).
- [6] J. H. Davis, *Biochim. Biophys. Acta* **737**, 117 (1983).
- [7] D. J. Semchyschyn and P. M. Macdonald, *Magn. Res. Chem.* **42**, 89 (2004).
- [8] H. U. Gally, G. Pluschke, P. Overath, and J. Seelig, *Biochemistry* **20**, 1826 (1981).
- [9] P. Scherer and J. Seelig, *EMBO J.* **6** (1987).
- [10] J. Seelig, *Cell Biology International Reports* **14**, 353 (1990), ISSN 0309-1651, URL <http://www.sciencedirect.com/science/article/pii/030916519091204H>.
- [11] R. Wohlgemuth, N. Waespe-Sarcevic, and J. Seelig, *Biochemistry* **19**, 3315 (1980).
- [12] G. Büldt and R. Wohlgemuth, *The Journal of Membrane Biology* **58**, 81 (1981), ISSN 1432-1424, URL <http://dx.doi.org/10.1007/BF01870972>.
- [13] A. Botan, F. Favela-Rosales, P. F. J. Fuchs, M. Javanainen, M. Kanduć, W. Kulig, A. Lamberg, C. Loison, A. Lyubartsev, M. S. Miettinen, et al., *J. Phys. Chem. B* **119**, 15075 (2015).
- [14] O. S. Ollila and G. Pabst, *Biochimica et Biophysica Acta (BBA) - Biomembranes* **1858**, 2512 (2016).
- [15] T. M. Ferreira, R. Sood, R. Bärenwald, G. Carlström, D. Topgaard, K. Saalwächter, P. K. J. Kinnunen, and O. H. S. Ollila, *Langmuir* **32**, 6524 (2016).
- [16] W. Pezeshkian, H. Khandelia, and D. Marsh, *Biophysical Journal* **114**, 1895 (2018), ISSN 0006-3495, URL <http://www.sciencedirect.com/science/article/pii/S0006349518302467>.
- [17] H. Akutsu, *Biochimica et Biophysica Acta (BBA) - Biomembranes* **1862**, 183352 (2020), URL <https://doi.org/10.1016/j.bbamem.2020.183352>.
- [18] H. M. Berman, J. Westbrook, Z. Feng, G. Gilliland, T. N. Bhat, H. Weissig, I. N. Shindyalov, and P. E. Bourne, *Nucleic Acids Research* **28**, 235 (2000), ISSN 0305-1048, <https://academic.oup.com/nar/article-pdf/28/1/235/9895144/280235.pdf>, URL <https://doi.org/10.1093/nar/28.1.235>.
- [19] D. Marsh and T. Páli, *European Biophysics Journal* **42**, 119 (2013), URL <https://doi.org/10.1007/s00249-012-0816-6>.
- [20] C. Sohlenkamp and O. Geiger, *FEMS Microbiology Reviews* **40**, 133 (2015).
- [21] J. E. Vance, *Traffic* **16**, 1 (2015).
- [22] E. Calzada, O. Onguka, and S. M. Claypool (Academic Press, 2016), vol. 321 of *International Review of Cell and Molecular Biology*, pp. 29 – 88.
- [23] D. Patel and S. N. Witt, *Oxidative Medicine and Cellular Longevity* **2017**, 4829180 (2017).
- [24] P. A. Leventis and S. Grinstein, *Annual Review of Biophysics* **39**, 407 (2010).
- [25] P. Hariharan, E. Tikhonova, J. Medeiros-Silva, A. Jeucken, M. V. Bogdanov, W. Dowhan, J. F. Brouwers, M. Weingarh, and L. Guan, *BMC Biology* **16**, 85 (2018).
- [26] P. L. Yeagle, *Biochimica et Biophysica Acta (BBA) - Biomembranes* **1838**, 1548 (2014), membrane Structure and Function: Relevance in the Cell's Physiology, Pathology and Therapy.
- [27] T. M. Ferreira, F. Coreta-Gomes, O. H. S. Ollila, M. J. Moreno, W. L. C. Vaz, and D. Topgaard, *Phys. Chem. Chem. Phys.* **15**, 1976 (2013).
- [28] S. V. Dvinskikh, H. Zimmermann, A. Maliniak, and D. Sandstrom, *J. Magn. Reson.* **168**, 194 (2004).
- [29] J. D. Gross, D. E. Warschawski, and R. G. Griffin, *J. Am. Chem. Soc.* **119**, 796 (1997).
- [30] M. Bak, J. T. Rasmussen, and N. C. Nielsen, *Journal of Magnetic Resonance* **147**, 296 (2000), ISSN 1090-7807, URL <http://www.sciencedirect.com/science/article/pii/S1090780700921797>.
- [31] H. S. Antila, P. Buslaev, F. Favela-Rosales, T. Mendes Ferreira, I. Gushchin, M. Javanainen, B. Kav, J. J. Madsen, J. Melcr,

- M. S. Miettinen, et al., The Journal of Physical Chemistry B p. acs.jpcc.9b06091 (2019), ISSN 1520-6106.
- [32] D. Marsh, *Handbook of Lipid Bilayers, Second Edition* (RSC press, 2013).
- [33] A. Catte, M. Girych, M. Javanainen, C. Loison, J. Melcr, M. S. Miettinen, L. Monticelli, J. Maatta, V. S. Oganessian, O. H. S. Ollila, et al., Phys. Chem. Chem. Phys. **18**, 32560 (2016).
- [34] J. L. Browning and J. Seelig, Biochemistry **19**, 1262 (1980).
- [35] F. Borle and J. Seelig, Chemistry and Physics of Lipids **36**, 263 (1985).
- [36] J. Seelig and H. U. Gally, Biochemistry **15**, 5199 (1976).
- [37] R. T. McGibbon, K. A. Beauchamp, M. P. Harrigan, C. Klein, J. M. Swails, C. X. Hernández, C. R. Schwantes, L.-P. Wang, T. J. Lane, and V. S. Pande, Biophysical Journal **109**, 1528 (2015).
- [38] P. G. Scherer and J. Seelig, Biochemistry **28**, 7720 (1989).
- [39] I. Pascher, M. Lundmark, P.-G. Nyholm, and S. Sundell, Biochim. Biophys. Acta **1113**, 339 (1992).
- [40] J. Seelig, P. M. MacDonald, and P. G. Scherer, Biochemistry **26**, 7535 (1987).
- [41] J. Melcr, T. M. Ferreira, P. Jungwirth, and O. H. S. Ollila, Journal of Chemical Theory and Computation **16**, 738 (2020).

ToDo

- | | P. |
|---|-----------|
| 1. How were α and γ -carbon peaks assigned in POPG? | 2 |
| 2. Details to be checked by Tiago | 2 |
| 4. This is to be finished once the final analysis is done as discussed in this issue: https://github.com/NMRLipids/NMRLipidsIVPEandPG/issues/40 | 2 |
| 3. This is a sketch, Tiago Ferreira will make a new figure. | 3 |
| 5. This part is to be finished once the analysis is finalized | 6 |